

A study on electro thermal response of SiC power module during high temperature operation

Tsuyoshi Funaki^{1a)}, Akira Nishio², Tsunenobu Kimoto,³
and Takashi Hikihara²

¹ Osaka University, Div. of Electrical, Electronic and Information Eng.
Graduate school of Engineering, Suita, Osaka 565-0871, Japan

² Kyoto University, Dept. of Electrical Eng.

³ Kyoto University, Dept. of Electronic Science and Eng.
Graduate school of Engineering, Katsura, Kyoto, 615-8510, Japan

^{a)}funaki@eei.eng.osaka-u.ac.jp

Abstract: This paper focuses on using high temperature operating capability of SiC power devices, which are packaged in power modules. A SiC Schottky barrier diode is mounted on an active metal brazed Si₃N₄ substrate as a heat resistive power module. The temperature dependency of electrical characteristics of the SiC device and thermal dynamics of the power module are modeled for numerical electro thermal analysis. The results of numerical analysis demonstrate high temperature operation of SiC device in the power module, which assumes less heat dissipation by simplified cooling system. The experimental results validate the numerical analysis results of the modeled SiC power module.

Keywords: temperature characteristics, SiC, power module, thermal distribution, thermal conduction

Classification: Electron devices

References

- [1] B. Jayant Baliga, *Silicon Carbide Power Devices*, World Scientific Pub Co. Inc., 2006.
- [2] T. Funaki, et al., "SiC JFET dc characteristics under extremely high ambient temperatures," *IEICE Electron. Express*, vol. 1, no. 17, pp. 523–527, 2004 .
- [3] T. Funaki, et al., "Switching characteristics of SiC JFET and Schottky diode in high-temperature dc-dc power converters," *IEICE Electron. Express*, vol. 2, no. 3, pp. 97–102, 2005.
- [4] J. Schulz-Harder, et al., "Advantages and New Development of DBC substrates," *Advancing Microelectronics*, vol. 32, no. 6, pp. 8–12, 2005.
- [5] S. M. Sze, *Physics of Semiconductor Devices (Second edition)*, New York: John Wiley & Sons, Inc., 1981.

- [6] Y. Cheng, et. al., *Electrothermal Analysis of VLSI Systems*, Kluwer Academic Pub., 2000.

1 Introduction

When they come into practical use, SiC power devices are expected to break conventional limitations of power electronics application, which stem from the material properties of Si [1]. High temperature operating capability of SiC devices is an advantageous characteristic compared to Si devices. The authors have been focusing on this feature, and evaluating the temperature dependency of the static and switching characteristics of the discrete SiC device [2, 3]. The conduction and switching loss in the device emanates heat, and must be radiated for safe operation. The high temperature operating ability of the SiC enables high density mounting in a power module with less elaborate cooling system. This results in power conversion systems with high power density. The high temperature power module can be realized using Si₃N₄ active metal brazed (AMB) substrates with high thermal conductivity and suitable coefficient of thermal expansion for SiC devices [4]. Heat management in a power module is a critical issue for high temperature operation, and an adequate numerical analysis model for electro thermal response of the power module is indispensable for evaluating its thermal response and distribution. First, the temperature dependency of the electrical characteristics of a SiC device, and the thermal characteristics of Si₃N₄ AMB power module substrate are characterized and modeled. Then they are synthesized in an electro thermal analysis model. The analysis results based on the proposed model are validated through a comparative study of numerical and experimental analysis results.

2 Modeling of SiC power module

The temperature dependency of electrical characteristics in a power device and thermal characteristics of the device package must be clarified for the coupled electro thermal analysis of the power module. This section models the electrical characteristics of a SiC device and the thermal response of the device package.

2.1 Temperature dependency of electrical characteristics of SiC SBD

The temperature dependency of the electrical characteristics of SiC SBD (Schottky barrier diode) was precisely characterized and studied for a wide temperature range in reference [4]. This subsection simply models the forward conduction current–voltage (I–V) characteristics of the studied SiC device to implement an electro thermal analysis of the power module. The studied SiC SBD has rated current and voltage of 20 A and 600 V with 2.6 × 2.6 mm die size (1.8 × 1.8 mm active area) and 0.37 mm thickness.

The measured forward conduction I–V characteristics of the SiC SBD are shown in Fig. 1 (a) for ambient temperatures ranging from 30 to 310°C. The measured result clearly shows the changes in knee voltage and gradient of the characteristics line with respect to the temperature. The I–V characteristics of the SBD and its temperature dependency can be modeled by eq. (1) [5].

$$V = \frac{kT}{e} \ln [A(T) I + 1] + B(T) I$$

$$\begin{cases} A(T) = \frac{\exp(\frac{e\phi}{kT})}{SA^*T^2} \\ B(T) = R_0 \{1 + \alpha(T - T_0) + \beta(T - T_0)^2\} \end{cases} \quad (1)$$

Here, k is the Boltzman constant, e is the unit charge, T is the temperature [K], ϕ is the barrier height [eV], S is the junction area [cm²], and A^* is the effective Recharadson constant.

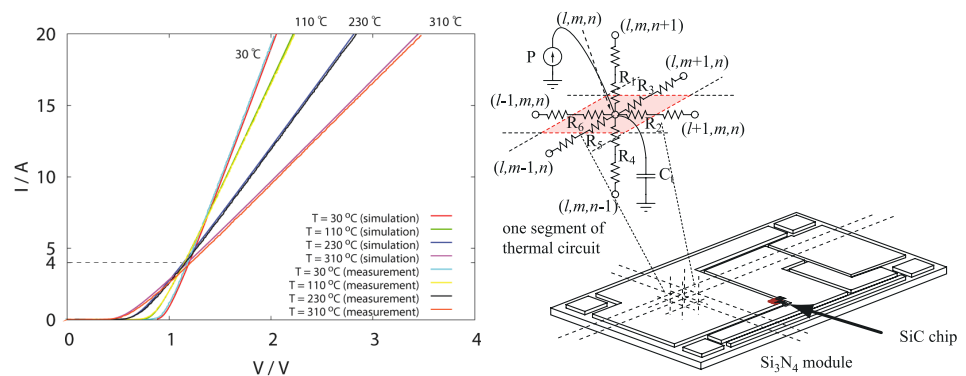
The first term in eq.(1) gives the Schottky junction characteristics. The second term represents the voltage drop at the effective series resistance in the device, which consists of resistance in drift region, contact, lead wire, etc; its temperature characteristics are expressed by a second order linear polynomial with reference temperature at $T_0 = 295$ K. The unknown parameters are identified from the measured results with least mean square method as $R_0 = 0.05015 \Omega$, $T_0 = 295$ K, $\alpha = 1.740 \times 10^{-3}$, and $\beta = 1.470 \times 10^{-5}$. The modeled I–V characteristics are also drawn in Fig. 1 (a). The modeled characteristic curves suitably coincide with the measured results for the respective temperature. Therefore, the model given by eq.(1) is validated for operation under a wide temperature range.

2.2 Thermal circuit of the device package

Heat conduction in a power module is governed by the heat diffusion equation (2). [6]

$$\rho c \frac{\partial T(x, y, z, t)}{\partial t} = \lambda \nabla^2 T(x, y, z, t) + g(x, y, z, t) \quad (2)$$

Here, ρ is the material density [kg/m³], c the specific heat [J/kg°C], λ the thermal conductivity [W/m°C], and g is the power density of the heat source



(a) I–V characteristics of the SiC SBD. (b) Thermal circuit model of the power module.

Fig. 1. SiC power module model.

[W/m³].

The studied power module is subjected to the thermal boundary condition of convective (Robin) conditions, resulting from the surrounding ambient condition of air cooling without a blower. The Robin condition is given as eq.(3).

$$-\lambda \frac{\partial T}{\partial s_i} = h (T - T_a). \quad (3)$$

Here, s_i is the outward direction, normal to surface i , h is the heat transfer coefficient, and T_a is the ambient temperature.

The Finite Difference Method is used in this paper to solve the heat conduction problem numerically. The thermal resistance $R_1, R_2, R_3, R_4, R_5, R_6$ and thermal capacitance C_t can be found by applying the first law of thermodynamics to the grid point (l, m, n) , as shown in Fig. 1 (b), and the relation is expressed by eq.(4).

$$\begin{aligned} & \frac{T_{l+1,m,n}^j - T_{l,m,n}^j}{R_1} + \frac{T_{l-1,m,n}^j - T_{l,m,n}^j}{R_4} + \frac{T_{l,m+1,n}^j - T_{l,m,n}^j}{R_2} + \frac{T_{l,m,n-1}^j - T_{l,m,n}^j}{R_5} \\ & + \frac{T_{l,m,n+1}^j - T_{l,m,n}^j}{R_3} + \frac{T_{l,m,n-1}^j - T_{l,m,n}^j}{R_6} \\ & = C_t \frac{T_{l,m,n}^{j+1} - T_{l,m,n}^j}{\Delta t} + (d_{x+} + d_{x-}) (d_{y+} + d_{y-}) (d_{z+} + d_{z-}) g (l, m, n, j \Delta t) \end{aligned} \quad (4)$$

$$\begin{aligned} R_1 &= \frac{2l_{x+}}{\lambda(l_{y+} + l_{y-})(l_{z+} + l_{z-})}, R_4 = \frac{2l_{x-}}{\lambda(l_{y+} + l_{y-})(l_{z+} + l_{z-})} \\ R_2 &= \frac{2l_{y+}}{\lambda(l_{x+} + l_{x-})(l_{z+} + l_{z-})}, R_5 = \frac{2l_{y-}}{\lambda(l_{x+} + l_{x-})(l_{z+} + l_{z-})} \\ R_3 &= \frac{2l_{z+}}{\lambda(l_{x+} + l_{x-})(l_{y+} + l_{y-})}, R_6 = \frac{2l_{z-}}{\lambda(l_{x+} + l_{x-})(l_{y+} + l_{y-})} \\ C_t &= (l_{x+} + l_{x-}) (l_{y+} + l_{y-}) (l_{z+} + l_{z-}) \rho c \end{aligned}$$

Here, $d_{x\pm}, d_{y\pm}, d_{z\pm}$ represent halves of the distance from grid (l, m, n) to grids $(l \pm 1, m, n), (l, m \pm 1, n), (l, m, n \pm 1)$, respectively, Δt is the time increment, and $T_{l,m,n}^j$ is the temperature at time $j \Delta t$.

The constants used for thermal conduction analysis are $\lambda = 400, \rho = 8930, c = 385$ for Cu, $\lambda = 370, \rho = 3210, c = 665$ for 4H-SiC, and $\lambda = 60, \rho = 3500, c = 600$ for Si₃N₄. The studied module is (H) 63.5 mm × (W) 35.5 mm × (T) 0.3 mm(Cu) + 0.4 mm(Si₃N₄) + 0.3 mm(Cu), and it is subdivided into grid structure by (H) 115 × (W) 64 × (T) 3 segments for numerical analysis. The heat transfer coefficient for a horizontal flat surface at the package is obtained experimentally as $h = 13.87P^{0.203}$. Here, P [W] is the total injected heat to the package.

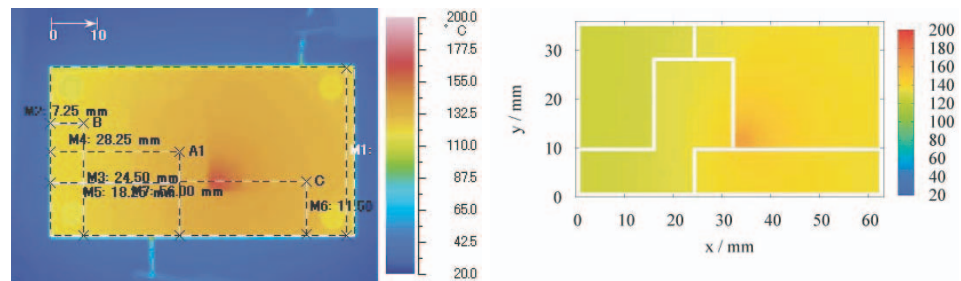
3 Experimental and numerical results

This section evaluates electrical and thermal response of the SiC power module numerically and experimentally. The dynamic change of thermal distribution in the power module is subject to heat injection from the device, conduction in the module, and dissipation to the ambient air. A step current of $I = 8$ A is imposed on the SiC SBD in the module. Figure 2 (a) shows the experimental results of thermal distribution of the module, measured from the opposite side of the module substrate, where the SiC SBD is mounted,

and the image of the dynamic response is presented with movie. The temperature was measured as the radiated infra-red rays with a thermo tracer camera (NEC-Sanei TH9100MLN). Figure 2 (b) gives the numerical results for Fig. 2 (a). Both the experimental and numerical results show that the temperature for the whole module rises with time, due to losses in the device. The temperature in the segment of the module where the SiC device is located gives the highest value, and the temperature gradient there is salient. The low temperature circles at the four corners in the experimental result are caused by the hole made to screwed the substrate down on a spacer. The temperature reaches 180°C. A rough change in thermal distribution is found along the edge of the electrical conduction layer, which is attributed to the difference in thermal conductance between the Cu conductor layer and Si₃N₄ insulating substrate. A comparative study and quantitative conformity of the thermal distribution validates the model of the electro thermal system of the power module with an equivalent electrical RC circuit, and confirms the high temperature operation of the SiC device.

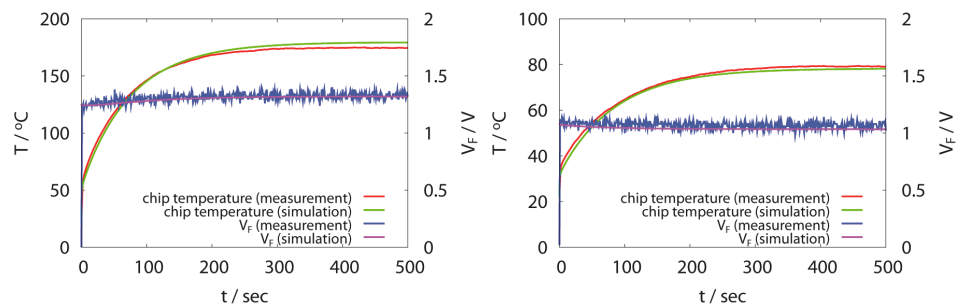
Figure 3 shows the time series response of the temperature and terminal voltage of the SiC SBD in the power module to the step current.

The temperature increases immediately after the application of step current and saturates around $t = 400$ sec. In Fig. 3 (a), although the measured temperature is less than the simulated result at the saturation temperature, the temperature difference is small for the high operating temperature of



(a) Experimental result. (b) Numerical result.

Fig. 2. The thermal distribution and time response in the SiC power module.



(a) I=8A (b) I=3A

Fig. 3. The temperature and terminal voltage response of SiC SBD in the power module.

180°C. The simulated temperature agrees more with the experimental results for lower temperatures of 80°C, with a smaller current, $I = 3$ A, as shown in Fig. 3 (b).

The voltage drop in the device for the same current ($I = 8$ A) became higher as the temperature increased, as shown in Fig. 1 (a). This is dynamically confirmed in Fig. 3 (a) by gradually increasing the forward voltage drop. The adverse phenomenon in the forward voltage drop occurs for $I = 3$ A, where the voltage drop for the same current is lowered as the temperature increases, as shown in Fig. 1 (a). The decrement of terminal voltage drop with time is confirmed in Fig. 3 (b). The numerical results of change in voltage drop shown in Figs. 3(a) and (b), coincide with the experimental results, in conjunction with the corresponding temperature response. Therefore, the proposed model is competent in its electro thermal analysis of the SiC power module in high temperature operation.

4 Conclusion

This paper experimentally and numerically assesses the thermal response and high temperature operating capability of an SiC power module. The temperature dependency of the electrical characteristics of the SiC SBD were characterized and modeled. The thermal circuit of the power module was also modeled as an equivalent electrical circuit. Then, the electro thermal analysis model was configured with an electrical circuit by synthesizing the electrical characteristics of the SiC device and equivalent thermal circuit. The thermal response of the power module to the applied current was evaluated as thermal imagery, and validated high temperature operation, both numerically and experimentally. The numerical result for electrical and thermal response is consistent with experimental results from room temperature to extremely high temperatures. Thus, the proposed electro thermal analysis model is applicable to the thermal design of SiC power modules, which are expected to operate over a wide temperature range.

This paper focused on precisely evaluating thermal response and distribution in the power module, then the number of subdivided grid of power module is quite large due to 3-D structure modeling, and the numerical computation time for the RC thermal circuit elements becomes tremendous. Therefore, this thermal circuit modeling approach is not attractive for analyzing the electrical response of the power module with multiple devices. Then, the future work will discuss the abbreviation of thermal circuit model into compact model with preserving the propriety of thermal response at the remarkable point.

Acknowledgments

This research was supported in part by the Ministry of Education, Culture, Sports, Sciences and Technology in Japan, the Grant-in-Aid for Scientific Research no. 17686024, 18360137, the 21st Century COE Program no. 14213201.